

Mottness-induced healing in strongly correlated superconductors

Shao Tang,¹ E. Miranda,² and V. Dobrosavljevic¹

¹*Department of Physics and National High Magnetic Field Laboratory,
Florida State University, Tallahassee, Florida 32306, USA*

²*Instituto de Física Gleb Wataghin, Campinas State University,
Rua Sérgio Buarque de Holanda, 777, CEP 13083-859, Campinas, Brazil*

We study impurity healing effects in models of strongly correlated superconductors. We show that in general both the range and the amplitude of the spatial variations caused by nonmagnetic impurities are significantly suppressed in the superconducting as well as in the normal states. We explicitly quantify the weights of the local and the non-local responses to inhomogeneities and show that the former are overwhelmingly dominant over the latter. We find that the local response is characterized by a well-defined healing length scale, which is restricted to only a few lattice spacings over a significant range of dopings in the vicinity of the Mott insulating state. We demonstrate that this healing effect is ultimately due to the suppression of charge fluctuations induced by Mottness. We also define and solve analytically a simplified yet accurate model of healing, within which we obtain simple expressions for quantities of direct experimental relevance.

PACS numbers: 71.10.Fd, 71.27.+a, 71.30.+h

Introduction.—Strong electronic correlations are believed to be essential for a complete understanding of many classes of unconventional superconductors, such as the cuprates [1–4], heavy fermion superconductors [5], organic materials [6, 7] and iron pnictides [8]. Among the many puzzling features of these systems is their behavior in the presence of disorder. In the case of the cuprates, experiments have shown that these d -wave superconductors are quite robust against disorder as introduced by carrier doping [3, 9, 10]. In particular, there seems to be a “quantum protection” of the d -wave nodal points [11]. Other anomalies were found in the organics [12] and the pnictides [13]. Although it is controversial whether conventional theory is able to explain these features [14], strong electronic interactions can give rise to these impurity screening effects. Indeed, they have been captured numerically by the Gutzwiller-projected wave function [15–17], even though a deeper insight into the underlying mechanism is still lacking. Similar impurity screening phenomena have been found as a result of strong correlations in the metallic state of the Hubbard model [18].

Despite this progress, it would be desirable to understand to what extent this disorder screening is due only to the presence of strong correlations or whether it is dependent on the details of the particular model or system. For example, are the effects of the inter-site super-exchange, crucial to describe the cuprates, essential for this phenomenon? To address these issues, it would be fruitful to have an analytical treatment of the problem. We will describe in this Letter how an expansion in the disorder potential is able to provide important insights into these questions. In particular, we show that the “healing” of the impurities is a sheer consequence of the strong correlations and depend very little on the symmetry of the superconducting (SC) state or the inclusion of inter-site magnetic correlations.

We considered dilute nonmagnetic impurities in an otherwise homogenous, strongly correlated electronic state. We avoided complications related to the nucleation of possible

different competing orders by the added impurities, such as fluctuating or static charge- and spin-density-waves [19–22] or the formation of local moments [23]. Therefore, we focused only on how a given strongly correlated state readjusts itself in the presence of the impurities. We used a spatially inhomogeneous slave boson treatment [4, 24–27], which allowed us to perform a complete quantitative calculation. We have allowed for either or both of d -wave SC and s -wave resonating valence bond (RVB) orders.

Our analytical and numerical results demonstrate that (i) for sufficiently weak correlations we recover the results of the conventional theory [14], in which the variations of the different fields induced by the impurities show oscillations with a long-ranged power-law envelope; (ii) for strong interactions and in several different broken symmetry states, the amplitude of the oscillations is strongly suppressed by a common pre-factor x , the deviation from half-filling; (iii) the spatial disturbances of the SC gap are healed over a precisely defined length scale, which does not exceed a few lattice parameters around the impurities; and (iv) this “healing effect” is intrinsically tied to the proximity to the Mott insulating state, even though it survives up to around 30% doping.

Model and method.—We study the $t - t' - J$ model on a cubic lattice in d dimensions with dilute nonmagnetic impurities

$$H = - \sum_{ij\sigma} t_{ij} c_{i\sigma}^\dagger c_{j\sigma} + J \sum_{ij} \mathbf{S}_i \cdot \mathbf{S}_j + \sum_i (\varepsilon_i - \mu_0) n_i, \quad (1)$$

where t_{ij} are the hopping matrix elements between nearest-neighbor (t) and second-nearest-neighbor (t') sites, $c_{i\sigma}^\dagger$ ($c_{i\sigma}$) is the creation (annihilation) operator of an electron with spin projection σ at site i , J is the super-exchange coupling constant between nearest-neighbor sites, $n_i = \sum_\sigma c_{i\sigma}^\dagger c_{i\sigma}$ is the number operator, μ_0 is the chemical potential and ε_i is the impurity potential. The no double occupancy constraint ($n_i \leq 1$) is implied. We set the nearest-neighbor hopping t as the energy unit and choose $t' = -0.25t$. To

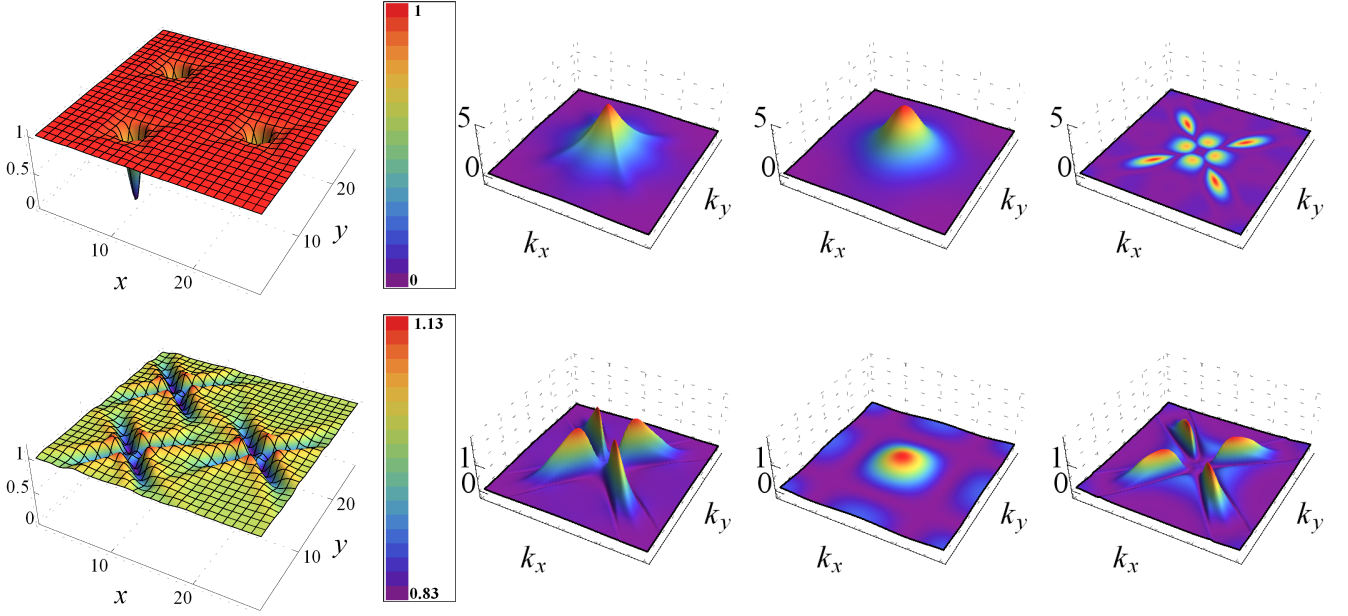


Figure 1: Spatial variations of normalized local SC gap $\frac{\Delta_i}{\Delta_0}$ for three impurities (first column) and the corresponding power spectra $S(\mathbf{k})$, $S(\mathbf{k})_{loc}$ and $S(\mathbf{k})_{nonloc}$ (second to fourth columns), in the presence (top) and in the absence (bottom) of correlations for $x = 0.2$. The strong suppression of gap oscillations by correlations can be traced to the dominance of the local, spherically symmetric power spectrum [$S_{loc}(\mathbf{k})$] over the non-local anisotropic part [$S_{nonloc}(\mathbf{k})$].

treat this model, we employ the $U(1)$ slave boson theory [4, 24, 26, 28]. Details can be found in [4] and we only describe it very briefly here. It starts with the replacement $c_{i\sigma}^\dagger = f_{i\sigma}^\dagger b_i$, where $f_{i\sigma}^\dagger$ and b_i are auxiliary fermionic (spinon) and bosonic fields, and the representation is faithful in the subspace $n_i \leq 1$ if the constraint $\sum_\sigma f_{i\sigma}^\dagger f_{i\sigma} + b_i^\dagger b_i = 1$ is enforced. This is implemented by a Lagrange multiplier λ_i on each site. The J term is then decoupled by Hubbard-Stratonovich fields in the particle-particle (Δ_{ij}) and particle-hole (χ_{ij}) channels. The auxiliary bosonic fields are all treated in the saddle-point approximation: $\langle b_i \rangle = r_i = \sqrt{Z_i}$ gives the quasiparticle residue, $\langle \lambda_i \rangle$ renormalizes the site energies and $\chi_{ij} = \sum_\sigma \langle f_{i\sigma}^\dagger f_{j\sigma} \rangle$ and $\Delta_{ij} = \langle f_{i\uparrow}^\dagger f_{j\downarrow} - f_{i\downarrow}^\dagger f_{j\uparrow} \rangle$ describe, respectively, the strength of a spinon singlet and the pairing amplitude across the corresponding bonds. Note that we do not assume these values are spatially uniform. This treatment is equivalent to the Gutzwiller approximation [2, 15]. In terms of Gorkov's spinor notation [29] with $\Psi_i(i\omega_n) = \begin{bmatrix} f_{i\uparrow}^\dagger(i\omega_n) & f_{i\downarrow}(-i\omega_n) \end{bmatrix}^\dagger$, where ω_n is the fermionic Matsubara frequency, the spinon Green's function is a 2×2 matrix: $[G_{ij}(i\omega_n)]_{ab} = -\langle \Psi_i(i\omega_n) \Psi_j^\dagger(i\omega_n) \rangle_{ab}$. Defining $h_{ij} \equiv -t_{ij}$, the saddle-point equations read as follows

$$\chi_{ij} = 2T \sum_n (G_{ij})_{11}, \quad (2)$$

$$\Delta_{ij} = -2T \sum_n (G_{ij})_{12}, \quad (3)$$

$$(r_i^2 - 1) = -2T \sum_n (G_{ii})_{11}, \quad (4)$$

$$\lambda_i r_i = -2T \sum_{nl} h_{il} r_l (G_{il})_{11} = -\sum_l h_{il} r_l \chi_{il}. \quad (5)$$

Note that we used Eq. (2) in the second equality of Eq. (5). At $T = 0$ and in the clean limit $\varepsilon_i = 0$, we have $Z = Z_0 = x$. The Mott metal-insulator transition is signaled by the vanishing of the quasi-particle weight $Z_0 \rightarrow 0$ at half-filling. It will be interesting to compare the results of the above procedure with the ones obtained from solving only Eqs. (2-3) while setting $Z_i = 1$ and $\lambda_i = 0$. The two sets will be called correlated and non-correlated, respectively. In order to be able to compare them, we set $J = t/3$ in the correlated case and adjusted J in the non-correlated case in such a way that the two clean dimensional SC gaps coincide, as discussed in reference [15].

Healing.— Although the detailed solutions of Eqs. (2-5) can be straightforwardly obtained numerically, we will focus on the case of weak scattering by dilute impurities and expand those equations up to first order in ε_i around the homogeneous case. It has been shown and we confirm that disorder induces long-ranged oscillations in various physical quantities, specially near the nodal directions in the d -wave SC state [14]. The linear approximation we employ is quite accurate for these extended disturbances far from the impurities, since these are always small. Besides, it provides more analytical insight into the results.

In general, we can expand the spatial variations of the various order parameters in different symmetry channels through

cubic harmonics: $\delta\varphi_{ij} = \sum_g \delta\varphi_i \Gamma(g)_{ij}$ where $\varphi_{ij} = \chi_{ij}$ or Δ_{ij} and $\Gamma(g)_{ij}$ are the basis functions for cubic harmonic g of the square lattice [33]. In the current discussion, we choose $\delta\chi_{ij} = \delta\chi_i \Gamma(s)_{ij}$ and $\delta\Delta_{ij} = \delta\Delta_i \Gamma(d_{x^2-y^2})_{ij}$, as we are interested in oscillations with the same symmetry as the ground state [4, 24, 26, 28]. We also assume there is no phase difference between order parameters on different bonds linked to same site. Then, we can define “local” spatial variations of the order parameters as $\delta\chi_i \equiv \frac{1}{2d} \sum_j \delta\chi_{ij} \Gamma(s)_{ij}$ and $\delta\Delta_i \equiv \frac{1}{2d} \sum_j \delta\Delta_{ij} \Gamma(d_{x^2-y^2})_{ij}$. Details of the calculation can be found in the Supplemental Material [30].

We find that both $\delta\chi_{ij}$ and $\delta\Delta_{ij}$, as well as the impurity-induced charge disturbance δn_i , are proportional to $Z_0 = x$, indicating the importance of strong correlations for the healing effect. Indeed, we can trace back this behavior to the readjustment of the r_i and λ_i fields, as encoded in Eqs. (4-5). Besides, this $\mathcal{O}(x)$ suppression is a generic consequence of the structure of the mean-field equations and holds for different broken symmetry states, such as the flux phase state, s -wave superconductivity, etc.

Let us focus in more detail on the spatial variations of the local pairing field $\delta\Delta_i$. In the first column of Fig. 1 we show results for $\delta\Delta_i$ for three identical impurities. The “cross-like” tails near the nodal directions [31] are conspicuous in the absence of correlations (bottom) but are strongly suppressed in their presence (top). While this suppression is further enhanced as the Mott metal-insulator transition is approached ($x \rightarrow 0$), it is still quite significant even at optimal doping ($x = 0.2$). This is the “healing” effect previously reported [15–17]. In order to gain insight into its underlying mechanism, we look at the spatial correlation function of local gap fluctuations

$$\left\langle \frac{\delta\Delta_i}{\Delta_0} \frac{\delta\Delta_j}{\Delta_0} \right\rangle_{disorder} = f(\mathbf{r}_i - \mathbf{r}_j), \quad (6)$$

where the brackets denote an average over disorder, after which lattice translation invariance is recovered. The Fourier transform of $f(\mathbf{r})$ can be written in the linear approximation as

$$f(\mathbf{k}) = \alpha W^2 S(\mathbf{k}), \quad (7)$$

where W is the disorder strength, α depends on the detailed bare disorder distribution, and the “power spectrum” (PS) $S(\mathbf{k})$ is related to gap linear response function $M_\Delta(\mathbf{k})$ by $S(\mathbf{k}) = M_\Delta^2(\mathbf{k})$. The latter is defined by Fourier transforming the kernel in $\delta\Delta_i = \Delta_0 \sum_j M_\Delta(\mathbf{r}_i - \mathbf{r}_j) \varepsilon_j$, which in turn can be easily obtained from the solution of the linearized equations [30]. Inspired by the strongly localized gap fluctuations at the top left of Fig. 1, we define the local component of the PS $S_{loc}(\mathbf{k}) \equiv M_{\Delta,loc}^2(\mathbf{k})$, where $M_{\Delta,loc}(\mathbf{k})$ is obtained by *restricting the lattice sums up to the second nearest neighbor distance* ($\sqrt{2}a$) in the linearized equations [30]. We also define $S_{nonloc}(\mathbf{k}) = M_{\Delta,nonloc}^2(\mathbf{k}) \equiv [M_\Delta(\mathbf{k}) - M_{\Delta,loc}(\mathbf{k})]^2$. In the last three columns of Fig. 1, we show, in this order, $S(\mathbf{k})$, $S_{loc}(\mathbf{k})$, and $S_{nonloc}(\mathbf{k})$ for the correlated (top) and non-

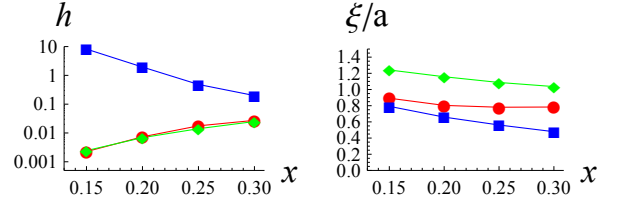


Figure 2: Left panel: the healing factor h as a function of doping in the uncorrelated case (blue curve with squares), in the correlated case (red curve with circles), and in the correlated case without $\delta\chi_i$ fluctuations (green curve with diamonds). Right panel: doping dependence of the SC (ξ_S , red curve with circles) and normal state (ξ_N , blue curve with squares) healing lengths. The green curve with diamonds gives ξ_S calculated within the minimal model (see text).

correlated (bottom) cases at $x = 0.2$. Clearly, in the presence of correlations the local PS is characterized by a smooth, spherically symmetric bell-shaped function, whereas the non-local part is highly anisotropic. Besides and more importantly, the non-local PS is negligibly small in the correlated case. The full PS is thus *overwhelmingly dominated* by the local part, unlike in the non-correlated case. In the Supplemental Material [30], we extend the analysis to the underdoped and overdoped regimes, where very similar behavior is found, even up to dopings of $x = 0.3$.

In order to quantify the localized nature of the healing effect, we are led to a natural definition of a “healing factor” h in the d -wave SC state

$$h = \frac{\int S_{nonloc}(\mathbf{k}) d^2k}{\int S_{loc}(\mathbf{k}) d^2k}, \quad (8)$$

where the integration is over the first Brillouin zone. It measures the relative weight of non-local and local parts of the gap PS. The healing factor as a function of doping is shown on the left panel of Fig. 2 for the non-correlated (blue) and correlated (red) cases. The contrast is striking. When correlations are present, h is extremely small up to 30% doping and the gap disturbance is restricted to a small area around the impurities. In contrast, without correlations significant pair fluctuations occur over quite a large area for all dopings shown. We conclude that the strong dominance of the local part over the highly anisotropic non-local contribution caused by correlations is the *key feature behind the healing process*.

The shape of $S_{loc}(\mathbf{k})$ shows that the gap disturbance created by an impurity is healed over a well-defined distance, the “healing length” ξ_S . This length scale can be obtained by expanding the inverse of $M_{\Delta,loc}(\mathbf{k})$ [or equivalently $M_\Delta(\mathbf{k})$] up to second order in k^2 , thus defining a Lorentzian in \mathbf{k} -space

$$M_{\Delta,loc}(\mathbf{k}) \approx \frac{1}{A + Bk^2}. \quad (9)$$

The SC healing length is then given by $\xi_S = \sqrt{B/A}$. The x dependence of ξ_S is shown in red on the right panel of Fig. 2. It is of the order of one lattice spacing in the relevant range

$0.15 < x < 0.3$. It should be noted that precisely the same length scale also governs the healing of charge fluctuations in the SC state, showing that this phenomenon is generic to the strongly correlated state. A similar procedure can be carried out for the charge fluctuations in the normal state, thus defining a normal state healing length ξ_N [30]. The blue curve of the right panel of Fig. 2 shows the x dependence of ξ_N , which is also of the order of one lattice spacing.

Mottness-induced healing.—The healing effect we have described comes almost exclusively from the δr_i and $\delta \lambda_i$ fluctuations: h is hardly affected by the $\delta \chi_i$ field. If we suppress the $\delta \chi_i$ fluctuations completely [30], there is only a tiny change in the results, as shown by the green curve of the left panel of Fig 2. The same is not true, however, if we turn off either δr_i or $\delta \lambda_i$ or both. We conclude that the healing effect in the d -wave SC state originates from the strong correlation effects alone, rather than the spinon correlations.

Within the linear approximation we are employing, all fluctuation fields ($\delta \Delta$, δr , etc.) are proportional, in \mathbf{k} -space, to the disorder potential $\varepsilon(\mathbf{k})$. Therefore, they are also proportional to each other. In particular, given the centrality of the strong correlation fields, it is instructive to write the gap fluctuations in terms of the slave boson fluctuations

$$\delta \Delta(\mathbf{k}) = -2\chi_{pc}(\mathbf{k}) r \delta r(\mathbf{k}) = \chi_{pc}(\mathbf{k}) \delta n(\mathbf{k}). \quad (10)$$

In the last equality, we used $n_i = 1 - r_i^2$, which enables us to relate two physically transparent quantities: the gap and the charge fluctuations. Indeed, this will provide crucial physical insight into the healing process. By focusing on the linear charge response to the disorder potential $\delta n(\mathbf{k}) = n_0 M_n(\mathbf{k}) \varepsilon(\mathbf{k})$, we can, in complete analogy with the gap fluctuations, define a PS for the spatial charge fluctuations, $N(\mathbf{k}) = M_n^2(\mathbf{k})$. This PS can also be broken up into local [$N_{loc}(\mathbf{k}) = M_{n,loc}^2(\mathbf{k})$] and non-local [$N_{nonloc}(\mathbf{k}) = [M_n(\mathbf{k}) - M_{n,loc}(\mathbf{k})]^2$] parts, as was done for the gap-fluctuation PS. These two contributions, obtained from the solution of the full linearized equations, are shown in Fig. 3. The charge PS in the correlated d -wave SC state is also characterized by a smooth, almost spherically symmetric local part and a negligibly small anisotropic non-local contribution. Note also the strong similarity between the local PS for gap (top row of Fig. 1) and charge fluctuations. This shows a strong connection between the gap and charge responses. Evidently, this is also reflected in real space, where the charge disturbance is healed in the same strongly localized fashion as the gap disturbance [30]. In fact, the local part of the charge response function $M_{n,loc}(\mathbf{k})$ can be shown to be well approximated by a Lorentzian [30] and we can write for small \mathbf{k}

$$\delta \Delta_{loc}(\mathbf{k}) \approx -\chi_{pc}(\mathbf{k}=0) \frac{8r^2/\lambda}{k^2 + \xi_S^{-2}} \varepsilon(\mathbf{k}), \quad (11)$$

where the SC healing length ξ_S can be expressed in terms of the Green's functions of the clean system [30]. The relations implied by Eqs. (10) and (11), as well as the doping depen-

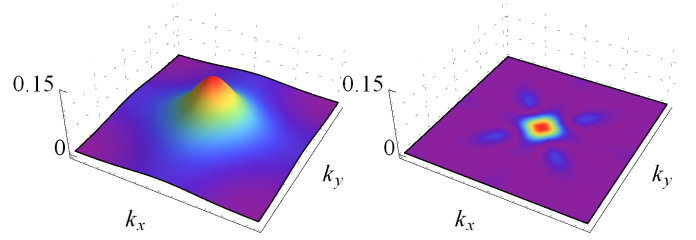


Figure 3: Local (left) and nonlocal (right) parts of the charge-fluctuation power spectra $N(\mathbf{k})_{loc}$ and $N(\mathbf{k})_{nonloc}$ in the presence of strong correlations for $x = 0.2$.

dence of the quantities in them, could be tested in STM studies and would constitute an important test of this theory.

Eqs. (10-11) allow us to obtain a clear physical picture of the healing mechanism. The spatial gap fluctuations can be viewed as being ultimately determined by the charge fluctuations. Furthermore, their ratio $\chi_{pc}(\mathbf{k})$, which is essentially a pair-charge correlation function, is a rather smooth function of order unity, only weakly renormalized by interactions. Therefore, it is the strong suppression of charge fluctuations by “Mottness”, as signaled by the r^2 factor in Eq. (11), which is behind the healing of gap fluctuations. This elucidates the physics of healing previously found numerically [15–17]. It also suggests that the healing phenomenon is generic to Mott systems [18] and is not tied to the specifics of the cuprates.

A minimal model.—Interestingly, the crucial role played by the strong correlation fields (r_i and λ_i) suggests a “minimal model” (MM) for an accurate description of the healing process, which we define as follows: (i) the spatially fluctuating strong correlation fields r_i and λ_i are first calculated for the self-consistently determined, fixed, uniform Δ and χ , and then (ii) the effects of their spatial readjustments are fed back into the gap equation (3) in order to find $\delta \Delta_i$ [30]. The accuracy of this procedure can be ascertained by the behavior of the healing factor: it is numerically indistinguishable from the green curve of the left panel of Fig. 2. Furthermore, the value of ξ_S calculated within the MM differs from the one obtained from the solution of the full linearized equations by at most 20% (red and green curves on the right panel of Fig. 2). Besides its accuracy, the advantage of this MM description lies in the simplicity of the analytical expressions obtained. As shown in the Supplemental Material [30], it provides simple expressions for the important quantities $\chi_{pc}(\mathbf{k})$ and ξ_S .

Conclusions.—In this work, we have found an inextricable link between the healing of gap and charge disturbances in strongly correlated superconductors, suggesting that this phenomenon is generic to any system close to Mott localization. An important experimental test of this link would be provided by STM studies of the organic superconductors [12] and maybe the pnictides [13]. Whether it is also relevant for heavy fermion systems [32] is an open question left for future study.

We acknowledge support by CNPq through grant 304311/2010-3 (EM), FAPESP through grant 07/57630-

5 (EM) and NSF through grant DMR-1005751 (ST and VD).

-
- [1] P. Anderson, *Science* **235**, 1196 (1987).
- [2] P. Anderson, P. Lee, M. Randeria, T. Rice, N. Trivedi, and F. Zhang, *J. Phys.: Condens. Matter* **16**, R755 (2004).
- [3] E. Dagotto, *Science* **309**, 257 (2005).
- [4] P. Lee, N. Nagaosa, and X. Wen, *Rev. Mod. Phys.* **78**, 17 (2006).
- [5] C. M. Varma, *Comments Solid State Phys.* **11**, 221 (1985).
- [6] B. J. Powell and R. H. McKenzie, *J. Phys.: Condens. Matter* **18**, R827 (2006).
- [7] B. J. Powell and R. H. McKenzie, *Rep. Prog. Phys.* **74**, 056501 (2011).
- [8] D. C. Johnston, *Adv. Phys.* **59**, 803 (2010).
- [9] K. McElroy, J. Lee, J. A. Slezak, D.-H. Lee, H. Eisaki, S. Uchida, and J. C. Davis, *Science* **309**, 1048 (2005).
- [10] K. Fujita, A. R. Schmidt, E.-A. Kim, M. J. Lawler, D. H. Lee, J. Davis, H. Eisaki, and S.-i. Uchida, *J. Phys. Soc. Jap.* **81**, 1005 (2012).
- [11] P. W. Anderson, *Science* **288**, 480 (2000).
- [12] J. G. Analytis, A. Ardavan, S. J. Blundell, R. L. Owen, E. F. Garman, C. Jeynes, and B. J. Powell, *Phys. Rev. Lett.* **96**, 177002 (2006).
- [13] J. Li, Y. F. Guo, S. B. Zhang, J. Yuan, Y. Tsujimoto, X. Wang, C. I. Sathish, Y. Sun, S. Yu, W. Yi, et al., *Phys. Rev. B* **85**, 214509 (2012).
- [14] A. Balatsky, I. Vekhter, and J. Zhu, *Rev. Mod. Phys.* **78**, 373 (2006).
- [15] A. Garg, M. Randeria, and N. Trivedi, *Nature Phys.* **4**, 762 (2008).
- [16] N. Fukushima, C.-P. Chou, and T. K. Lee, *J. Phys. Chem. Solids* **69**, 3046 (2008).
- [17] N. Fukushima, C.-P. Chou, and T. K. Lee, *Phys. Rev. B* **79**, 184510 (2009).
- [18] E. C. Andrade, E. Miranda, and V. Dobrosavljević, *Phys. Rev. Lett.* **104**, 236401 (2010).
- [19] E. Fradkin and S. A. Kivelson, *Nature Phys.* **8**, 864 (2012).
- [20] G. Ghiringhelli, M. Le Tacon, M. Minola, S. Blanco-Canosa, C. Mazzoli, N. B. Brookes, G. M. De Luca, A. Frano, D. G. Hawthorn, F. He, et al., *Science* **337**, 821 (2012).
- [21] A. C. Fang, L. Capriotti, D. J. Scalapino, S. A. Kivelson, N. Kaneko, M. Greven, and A. Kapitulnik, *Phys. Rev. Lett.* **96**, 017007 (2006).
- [22] M. Ubbens and P. Lee, *Phys. Rev. B* **46**, 8434 (1992).
- [23] H. Alloul, J. Bobroff, M. Gabay, and P. Hirschfeld, *Rev. Mod. Phys.* **81**, 45 (2009).
- [24] P. Coleman, *Phys. Rev. B* **29**, 3035 (1984).
- [25] G. Kotliar and A. Ruckenstein, *Phys. Rev. Lett.* **57**, 1362 (1986).
- [26] G. Kotliar and J. Liu, *Phys. Rev. B* **38**, 5142 (1988).
- [27] P. A. Lee, N. Nagaosa, T.-K. Ng, and X.-G. Wen, *Phys. Rev. B* **57**, 6003 (1998).
- [28] A. E. Ruckenstein, P. J. Hirschfeld, and J. Appel, *Phys. Rev. B* **36**, 857 (1987).
- [29] A. Abrikosov, L. Gorkov, and I. Dzyaloshinski, *Methods of quantum field theory in statistical physics* (Courier Dover Publications, 1975).
- [30] See the Supplemental Material at <http://link.aps.org/supplemental/XXXXX>.
- [31] A. V. Balatsky and M. I. Salkola, *Phys. Rev. Lett.* **76**, 2386 (1996).
- [32] J. Figgins and D. K. Morr, *Phys. Rev. Lett.* **107**, 066401 (2011).
- [33] s , $d_{x^2-y^2}$, d_{xy} , etc., with basis functions expressed as: $\cos k_x + \cos k_y$, $\cos k_x - \cos k_y$ and $\sin k_x \sin k_y$, etc.

Mottness-induced healing in strongly correlated superconductors: supplemental material

Shao Tang,¹ E. Miranda,² and V. Dobrosavljevic¹

¹*Department of Physics and National High Magnetic Field Laboratory,
Florida State University, Tallahassee, Florida 32306, USA*

²*Instituto de Física Gleb Wataghin, Campinas State University,
Rua Sérgio Buarque de Holanda, 777, CEP 13083-859, Campinas, Brazil*

PACS numbers: 71.10.Fd, 71.27.+a, 71.30.+h

I. THE LINEAR APPROXIMATION

Our linear approximation approach consists of expanding the mean-field equations (2-5) of the main text to first order in the site energies ε_i . Denoting linear deviations in the various fields by δ we get

$$\begin{aligned} \delta\chi_{ij} = & 2kT \sum_{nl} (-g_{il}g_{lj} + G_{1il}G_{1lj}) (\delta\lambda_l + \varepsilon_l) + 2kTr \sum_{nlm} (-g_{il}g_{mj} + G_{1il}G_{1mj}) (\delta r_l h_{lm} + \delta r_m h_{lm}) \\ & - 2kT \sum_{nlm} (-g_{il}g_{mj} + G_{1il}G_{1mj}) \left(\tilde{J}\delta\chi_{lm} \right) + 2kT \sum_{nlm} (g_{il}G_{1mj} + g_{mj}G_{1il}) \left(\tilde{J}\delta\Delta_{lm} \right), \end{aligned} \quad (1)$$

$$\begin{aligned} \delta\Delta_{ij} = & -2kT \sum_{nl} (g_{il}G_{1lj} + g_{lj}G_{1il}) (\delta\lambda_l + \varepsilon_l) - 2kTr \sum_{nlm} (g_{il}G_{1mj} + g_{mj}G_{1il}) (\delta r_l h_{lm} + \delta r_m h_{lm}) \\ & + 2kT \sum_{nlm} (g_{il}G_{1mj} + g_{mj}G_{1il}) \left(\tilde{J}\delta\chi_{lm} \right) - 2kT \sum_{nlm} (G_{1il}G_{2mj} + g_{il}g_{mj}) \left(\tilde{J}\delta\Delta_{lm} \right), \end{aligned} \quad (2)$$

$$\begin{aligned} -r\delta r_i = & kT \sum_{nl} (-g_{il}g_{li} + G_{1il}G_{1li}) (\delta\lambda_l + \varepsilon_l) + kTr \sum_{nlm} (-g_{il}g_{mi} + G_{1il}G_{1mi}) (\delta r_l h_{lm} + \delta r_m h_{lm}) \\ & - kT \sum_{nlm} (-g_{il}g_{mi} + G_{1il}G_{1mi}) \left(\tilde{J}\delta\chi_{lm} \right) + kT \sum_{nlm} (g_{il}G_{1mi} + g_{mi}G_{1il}) \left(\tilde{J}\delta\Delta_{lm} \right), \end{aligned} \quad (3)$$

$$\lambda\delta r_i + r\delta\lambda_i + \sum_l h_{il}\chi_{il}\delta r_l + r \sum_l h_{il}\delta\chi_{il} = 0, \quad (4)$$

where $G_{1ij} \equiv [G_{ij}]_{11}$, $G_{2ij} \equiv [G_{ij}]_{22}$, $g_{ij} \equiv [G_{ij}]_{12} = [G_{ij}]_{21}$ are the Green's functions of the clean system, n is the fermionic Matsubara frequency index and $\tilde{J} = \frac{3}{8}J$. The latter choice is made, in the presence of correlations, so that the multi-channel Hubbard-Stratonovich transformation we used reproduces, at the saddle-point level, the mean-field results [1][2]. In general, the clean Green's functions in \mathbf{k} -space are given by

$$G_1(\omega_n, \mathbf{k}) = \frac{i\omega_n + e(\mathbf{k})}{(i\omega_n)^2 - e^2(\mathbf{k}) - \tilde{J}^2\Delta^2(\mathbf{k})}, \quad (5)$$

$$G_2(\omega_n, \mathbf{k}) = \frac{i\omega_n - e(\mathbf{k})}{(i\omega_n)^2 - e^2(\mathbf{k}) - \tilde{J}^2\Delta^2(\mathbf{k})}, \quad (6)$$

$$g(\omega_n, \mathbf{k}) = \frac{\tilde{J}\Delta(\mathbf{k})}{(i\omega_n)^2 - e^2(\mathbf{k}) - \tilde{J}^2\Delta^2(\mathbf{k})}, \quad (7)$$

where the renormalized dispersion is

$$e(\mathbf{k}) = -2 \left(xt + \chi \tilde{J} \right) [\cos(k_x a) + \cos(k_y a)] - 4xt' \cos(k_x a) \cos(k_y a) - \mu, \quad (8)$$

we have absorbed the clean λ in the chemical potential, and

$$\Delta(\mathbf{k}) = 2\Delta_0 [\cos(k_x a) - \cos(k_y a)]. \quad (9)$$

Notice that the dimensionful gap function is $\Delta_{phys}(\mathbf{k}) = \tilde{J}\Delta(\mathbf{k})$. As we focus on the asymptotic long-range behavior of the different fields, their variations are dominated by the corresponding clean-limit symmetry channel. We therefore define local order parameters as $\delta\chi_i \equiv \frac{1}{2d} \sum_j \delta\chi_{ij} \Gamma(s)_{ij}$, $\delta\Delta_i \equiv \frac{1}{2d} \sum_j \delta\Delta_{ij} \Gamma(d_{x^2-y^2})_{ij}$. Thus, *defining vectors and matrices in the lattice site basis with bold-face letters*, Eqs. (1-4) can be recast as

$$(\mathbf{A} + r^2 \mathbf{B}) \delta\Phi = r^2 \mathbf{C}, \quad (10)$$

where

$$\mathbf{A} = \begin{pmatrix} M_{11} & M_{12} & M_{13} & M_{14} \\ M_{21} & M_{22} & M_{23} & M_{24} \\ M_{31} & M_{32} & M_{33} & M_{34} \\ 0 & 0 & \lambda \mathbf{1} - \frac{\lambda}{2d} \Gamma(s) & 0 \end{pmatrix}, \mathbf{B} = \begin{pmatrix} 0 & 0 & 0 & 0 \\ 0 & 0 & 0 & 0 \\ 0 & 0 & 0 & 0 \\ -2dt \mathbf{1} & 0 & 0 & \mathbf{1} \end{pmatrix}, \delta\Phi = \begin{pmatrix} \delta\chi \\ \delta\Delta \\ r\delta\mathbf{r} \\ \delta\bar{\lambda} \end{pmatrix}, \mathbf{C} = \begin{pmatrix} 0 \\ 0 \\ 0 \\ \boldsymbol{\varepsilon} \end{pmatrix}. \quad (11)$$

Here, the elements of (the vector) $\boldsymbol{\varepsilon}$ are the disorder potential values ε_i , $\mathbf{1}$ is the identity matrix, $\delta\bar{\lambda}_i = \delta\lambda_i + \varepsilon_i$, and

$$M_{11ij} = -\delta_{ij} - \frac{\tilde{J}kT}{d} \sum_{nml} \Gamma(s)_{il} (-g_{ij}g_{ml} + G_{1ij}G_{1ml}) \Gamma(s)_{jm} \quad (12)$$

$$M_{12ij} = \frac{\tilde{J}kT}{d} \sum_{nml} \Gamma(s)_{il} (g_{ij}G_{1ml} + g_{ml}G_{1ij}) \Gamma(d_{x^2-y^2})_{jm} \quad (13)$$

$$M_{13ij} = \frac{kT}{d} \sum_{nml} \Gamma(s)_{il} (-g_{ij}g_{ml} + G_{1ij}G_{1ml} - g_{im}g_{jl} + G_{1im}G_{1jl}) h_{jm} \quad (14)$$

$$M_{14ij} = \frac{kT}{d} \sum_{nl} \Gamma(s)_{il} (-g_{ij}g_{jl} + G_{1ij}G_{1jl}) \quad (15)$$

$$M_{21ij} = -\frac{\tilde{J}kT}{d} \sum_{nml} \Gamma(d_{x^2-y^2})_{il} (g_{ij}G_{1ml} + g_{ml}G_{1ij}) \Gamma(s)_{jm} \quad (16)$$

$$M_{22ij} = \delta_{ij} + \frac{\tilde{J}kT}{d} \sum_{nml} \Gamma(d_{x^2-y^2})_{il} (G_{1ij}G_{2ml} + g_{ij}g_{ml}) \Gamma(d_{x^2-y^2})_{jm} \quad (17)$$

$$M_{23ij} = \frac{kT}{d} \sum_{nml} \Gamma(d_{x^2-y^2})_{il} (g_{ij}G_{1ml} + g_{ml}G_{1ij} + g_{im}G_{1jl} + g_{jl}G_{1im}) h_{jm} \quad (18)$$

$$M_{24ij} = \frac{kT}{d} \sum_{nl} \Gamma(d_{x^2-y^2})_{il} (g_{ij}G_{1jl} + g_{jl}G_{1ij}) \quad (19)$$

$$M_{31ij} = -\tilde{J}kT \sum_{nm} (-g_{ij}g_{mi} + G_{1ij}G_{1mi}) \Gamma(s)_{jm} \quad (20)$$

$$M_{32ij} = \tilde{J}kT \sum_{nm} (g_{ij}G_{1mi} + g_{mi}G_{1ij}) \Gamma(d_{x^2-y^2})_{jm} \quad (21)$$

$$M_{33ij} = \delta_{ij} + kT \sum_{nm} h_{jm} (-g_{ij}g_{mi} + G_{1ij}G_{1mi} - g_{im}g_{ji} + G_{1im}G_{1ji}) \quad (22)$$

$$M_{34ij} = kT \sum_n (-g_{ij}g_{ji} + G_{1ij}G_{1ji}) \quad (23)$$

In writing Eqs. (10), we have made explicit the r dependence of Eqs. (1-4). We note, however, that there is also an implicit dependence on r through the dispersion (8) (where $x = r^2$), which enters the various Green's functions in Eqs. (5-7).

Since the matrix elements in Eqs. (12-23) are all calculated in the *translation-invariant clean system*, Eqs. (10) can be easily solved in \mathbf{k} -space by matrix inversion. Normal state results are obtained by removing the second row and column and setting $\Delta(\mathbf{k})$ to zero. Non-correlated results correspond to the absence of slave bosons and constraints, so we just remove the third and fourth rows and columns and set $x = 1$ and $\lambda_i = 0$. In every case, the clean limit is first solved self-consistently for χ , Δ , λ and μ , and then the fluctuations in the presence of impurities are obtained.

In discussing the solution to Eqs. (10), we rely on the fact that all quantities in Eqs. (12-23) are non-singular and finite as $x \rightarrow 0$. Thus, we can write their formal solution as

$$\delta\Phi = r^2 (\mathbf{A} + r^2\mathbf{B})^{-1} \mathbf{C} = r^2\mathbf{A}^{-1}\mathbf{C} + \mathcal{O}(r^4). \quad (24)$$

It follows that $\delta\chi_i$, $\delta\Delta_i$, $r\delta r_i$, and $\delta\bar{\lambda}_i = \delta\lambda_i + \varepsilon_i$ are all of order $r^2 = x$.

II. THE GAP FLUCTUATIONS AND THE HEALING FACTOR

In order to characterize quantitatively the healing process in the SC state, we focused on the linear gap response to the disorder potential

$$\delta\Delta_i = \Delta_0 \sum_j M_\Delta(\mathbf{r}_i - \mathbf{r}_j) \varepsilon_j, \quad (25)$$

which is obtained directly from the second line of the solution to Eqs. (24). In order to gain further insight, we separated the local and non-local parts of the gap response as follows. In Eqs. (10) as defined in real space, we separate sums over sites into a local part, with sums up to next-to-nearest neighbors (denoted by $r_{ij} \leq \sqrt{2}a$), and a non-local part, with sums over the remaining sites (denoted by $r_{ij} > \sqrt{2}a$). For example,

$$\sum_j M_{11ij} \delta\chi_j = \sum_{j, r_{ij} \leq \sqrt{2}a} M_{11ij} \delta\chi_j + \sum_{j, r_{ij} > \sqrt{2}a} M_{11ij} \delta\chi_j, \text{ etc.} \quad (26)$$

After solving the equations, this separation naturally defines local and non-local responses of the various fields. In \mathbf{k} -space, we can write

$$M_\Delta(\mathbf{k}) = M_{\Delta,loc}(\mathbf{k}) + M_{\Delta,nonloc}(\mathbf{k}). \quad (27)$$

This procedure is equivalent to projecting the full response in \mathbf{k} -space onto some lattice symmetry channels with different ranges: $\Gamma_s(\mathbf{k}) = 2[\cos(k_x a) + \cos(k_y a)]$ for nearest neighbors, and so on. Then, the power spectrum of spatial gap fluctuations follows naturally from this separation

$$S(\mathbf{k}) = M_\Delta^2(\mathbf{k}), \quad (28)$$

$$S_{loc}(\mathbf{k}) = M_{\Delta,loc}^2(\mathbf{k}), \quad (29)$$

$$S_{nonloc}(\mathbf{k}) = [M_\Delta(\mathbf{k}) - M_{\Delta,loc}(\mathbf{k})]^2. \quad (30)$$

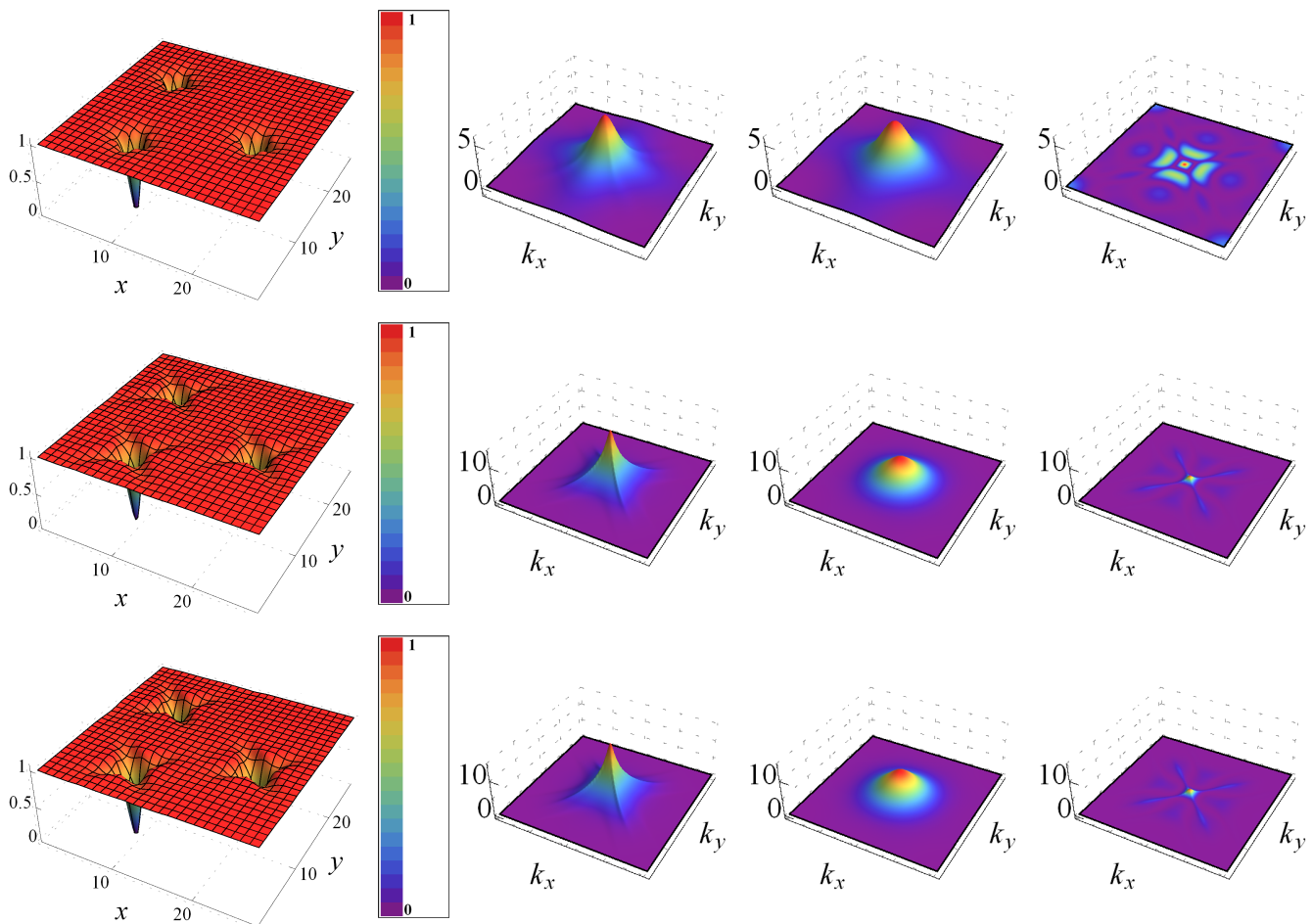


Figure 1: Spatial variations of normalized local gap function $\frac{\delta\Delta_i}{\Delta_0}$ for three impurities (first column) and the corresponding power spectra $S(\mathbf{k})$, $S(\mathbf{k})_{loc}$ and $S(\mathbf{k})_{nonloc}$ (second to fourth columns) for $x = 0.15$ (first row), $x = 0.25$ (second row), and $x = 0.3$ (third row). The corresponding healing factors are (a) $h = 0.23\%$, (b) $h = 1.77\%$, and (c) $h = 2.74\%$.

Finally, we define the healing factor as the ratio of integrated non-local to local contributions to the power spectrum

$$h = \frac{\int S_{nonloc}(\mathbf{k}) d^2k}{\int S_{loc}(\mathbf{k}) d^2k}. \quad (31)$$

The gap fluctuations $\delta\Delta_i$ for three impurities and power spectra, for several dopings and in the presence of correlations, are shown in Fig. 1. The strong healing in the presence of correlations is conspicuous. It is important to note that this suppression of gap fluctuations is not restricted to small dopings and remains quite strong even at $x = 0.3$, where the healing factor does not exceed 3%. As explained in the main text, the healing effect originates in the dominance of the local spherically symmetric part (third column in Fig. 1) over the anisotropic non-local response (fourth column in Fig. 1).

III. THE IRRELEVANCE OF SPINON FLUCTUATIONS AND THE “MINIMAL MODEL”

We can shed light on the strong healing effect by studying a simplified case obtained by “turning off” the $\delta\chi_i$ fluctuations. In this case, we need to solve the smaller set of equations

$$\begin{pmatrix} M_{22} & M_{23} & M_{24} \\ M_{32} & M_{33} & M_{34} \\ 0 & \lambda\mathbf{1} - \frac{\lambda}{2d}\mathbf{\Gamma}(s) & r^2\mathbf{1} \end{pmatrix} \begin{pmatrix} \delta\Delta \\ r\delta\mathbf{r} \\ \delta\bar{\lambda} \end{pmatrix} = \begin{pmatrix} 0 \\ 0 \\ r^2\boldsymbol{\varepsilon} \end{pmatrix}. \quad (32)$$

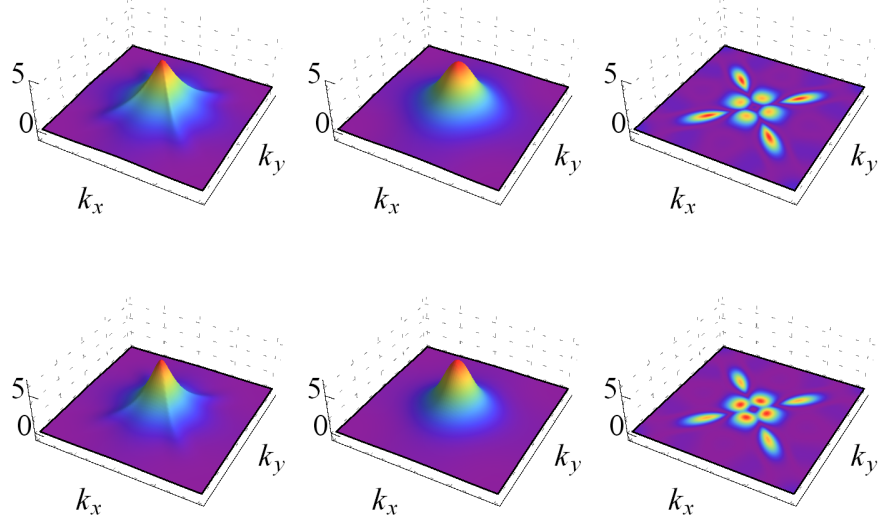


Figure 2: Power spectra of gap fluctuations $S(\mathbf{k})$, $S(\mathbf{k})_{loc}$ and $S(\mathbf{k})_{nonloc}$ (first to third columns) for $x = 0.2$ in the presence of correlations. The top figures were obtained from the full solution of the linearized Eqs. (10), whereas the bottom ones correspond to the minimal model (Eqs. (34)). Note that the healing factors are $h = 0.74\%$ (top) and $h = 0.69\%$ (bottom).

The healing factor obtained in this simplified model is almost identical to the full solution, as shown by the red and green curves of the left panel of Fig. 2 of the main text. This shows that the spinon field fluctuations are utterly irrelevant for the strong healing.

A further fruitful simplification is obtained by setting M_{32} to zero in Eqs. (32). This defines what we called the “minimal model” (MM). In this case, the “strong-correlation sub-block” of δr_i and $\delta \bar{\lambda}_i$ fluctuations decouples and suffers no feed-back from the gap fluctuations. In fact, the MM corresponds to breaking up the solution to the problem into two parts: (i) the spatially fluctuating strong correlation fields r_i and λ_i are first calculated for *fixed*, *uniform* Δ and χ , and then (ii) the effects of their spatial readjustments are fed back into the gap equation to find $\delta \Delta_i$.

Strikingly, the healing factor in this case is *numerically indistinguishable* from the one obtained from Eqs. (32) (green curve of the left panel of Fig. 2 of the main text). Furthermore, the full, local and non-local PS of gap fluctuations are also captured quite accurately by the MM, as seen in Fig. 2. We conclude that the MM, which incorporates only the effects of strong correlations, is able to describe with very high accuracy the healing process in the d -wave SC state.

The MM also permits us to obtain simple and physically transparent expressions. In particular, it follows immediately that

$$r\delta r(\mathbf{k}) = \frac{r^2}{\lambda a(\mathbf{k}) - r^2 M_{33}(\mathbf{k}) / M_{34}(\mathbf{k})} \varepsilon(\mathbf{k}), \quad (33)$$

where $a(\mathbf{k}) = 1 - \Gamma_s(\mathbf{k})/4$, and we used the Fourier transform of $\Gamma(s)$, $\Gamma_s(\mathbf{k}) = 2[\cos(k_x a) + \cos(k_y a)]$. Moreover,

$$\delta \Delta(\mathbf{k}) = \frac{r^2 [M_{24}(\mathbf{k}) M_{33}(\mathbf{k}) - M_{23}(\mathbf{k}) M_{34}(\mathbf{k})]}{M_{22}(\mathbf{k}) [\lambda a(\mathbf{k}) M_{34}(\mathbf{k}) - r^2 M_{33}(\mathbf{k})]} \varepsilon(\mathbf{k}), \quad (34)$$

$$= \frac{\left[M_{24}(\mathbf{k}) \frac{M_{33}(\mathbf{k})}{M_{34}(\mathbf{k})} - M_{23}(\mathbf{k}) \right]}{M_{22}(\mathbf{k})} r\delta r(\mathbf{k}). \quad (35)$$

$$= \chi_{pc}^{MM}(\mathbf{k}) \delta n(\mathbf{k}), \quad (36)$$

where we used $n_i = 1 - r_i^2 \Rightarrow \delta n_i = -2r\delta r_i$, and

$$\chi_{pc}^{MM}(\mathbf{k}) = -\frac{\left[M_{24}(\mathbf{k}) \frac{M_{33}(\mathbf{k})}{M_{34}(\mathbf{k})} - M_{23}(\mathbf{k}) \right]}{2M_{22}(\mathbf{k})}. \quad (37)$$

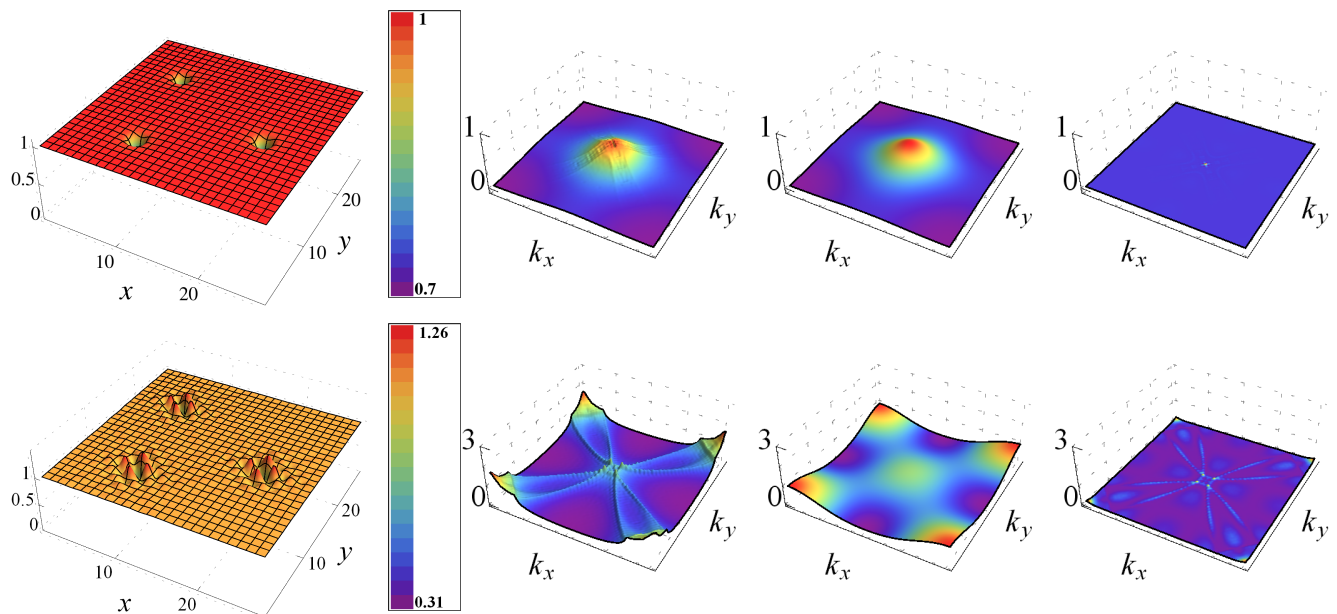


Figure 3: Spatial variations of normalized local density $\frac{\delta n_i}{n_0}$ in the normal state for three impurities (first column) and the corresponding power spectra $N(\mathbf{k})$, $N(\mathbf{k})_{loc}$ and $N(\mathbf{k})_{nonloc}$ (second to fourth columns), in the presence (top) and in the absence (bottom) of strong correlations for $x = 0.2$. The strong suppression of density oscillations by correlations is accompanied by the dominance of the spherically symmetric local power spectrum [$N_{loc}(\mathbf{k})$] over the anisotropic non-local one [$N_{nonloc}(\mathbf{k})$].

The local part of the response, which we have shown to be the dominant one, can be studied by looking at the long wavelength limit. As $k \rightarrow 0$, $a(\mathbf{k}) \sim k^2/4$ and

$$\delta\Delta_{loc}(\mathbf{k}) \approx -\chi_{pc}^{MM}(\mathbf{k}=0) \frac{8r^2/\lambda}{k^2 + \xi_S^{-2}} \varepsilon(\mathbf{k}), \quad (38)$$

where

$$\frac{1}{\xi_S} = \sqrt{-\frac{4r^2}{\lambda} \frac{M_{33}(\mathbf{k}=0)}{M_{34}(\mathbf{k}=0)}}. \quad (39)$$

Eqs. (37) and (39) give us the expressions for the pair-charge correlation function and the healing length within the MM.

IV. THE NORMAL STATE AND THE “MINIMAL MODEL”

It is instructive to analyze also the behavior of the charge fluctuations in the normal state. This can be achieved by suppressing the second row and column of Eqs. (10) and setting $\Delta(\mathbf{k})$, and thus $g(i\omega_n, \mathbf{k})$, to zero. Even after these simplifications, the full solution is long and cumbersome. However, accurate insight can be gained from a MM of the normal state, in which we also set the $\delta\chi_i$ to zero by hand. As before, the strong-correlation sub-block decouples and Eq. (33) is still valid (albeit with matrix elements calculated in the normal state). The local part of the charge response is given by an expression similar to Eq. (38)

$$\delta n_{loc}(\mathbf{k}) \approx -\frac{8r^2/\lambda}{k^2 + \xi_N^{-2}} \varepsilon(\mathbf{k}), \quad (40)$$

where ξ_N is given by Eq. (39), again with matrix elements calculated in the normal state. The behavior of ξ_N as a function of doping is shown by the green curve of the right panel of Fig. 2 of the main text.

In addition, just like in the Coulomb gas, the density fluctuations also show Friedel-like oscillations coming from the singularity in the response function at $2k_F$. Thus, expanding Eq. (33) in r^2 ,

$$\delta n_{nonloc}(|\mathbf{k}| \approx 2k_F) \approx -\frac{2r^2}{\lambda a(|\mathbf{k}| \approx 2k_F)} \left[1 + \frac{r^2 M_{33}(|\mathbf{k}| \approx 2k_F) / M_{34}(|\mathbf{k}| \approx 2k_F)}{\lambda a(|\mathbf{k}| \approx 2k_F)} \right] \varepsilon(\mathbf{k}). \quad (41)$$

Since

$$M_{34}(\mathbf{k}) = \mathbf{\Pi}(\mathbf{k}), \quad (42)$$

$$M_{33}(\mathbf{k}) = 1 + \mathbf{\Pi}^b(\mathbf{k}), \quad (43)$$

$$\mathbf{\Pi}(\mathbf{k}) = \frac{1}{V} \sum_{\mathbf{q}} \frac{f[\tilde{h}(\mathbf{q} + \mathbf{k})] - f[\tilde{h}(\mathbf{q})]}{\tilde{h}(\mathbf{q} + \mathbf{k}) - \tilde{h}(\mathbf{q})}, \quad (44)$$

$$\mathbf{\Pi}^b(\mathbf{k}) = \frac{1}{V} \sum_{\mathbf{q}} \frac{f[\tilde{h}(\mathbf{q} + \mathbf{k})] - f[\tilde{h}(\mathbf{q})]}{\tilde{h}(\mathbf{q} + \mathbf{k}) - \tilde{h}(\mathbf{q})} [h(\mathbf{q} + \mathbf{k}) + h(\mathbf{q})], \quad (45)$$

$$h(\mathbf{k}) = -t\Gamma_s(\mathbf{k}) - 4t' \cos(k_x a) \cos(k_y a), \quad (46)$$

the leading divergent behavior is

$$\frac{M_{33}(|\mathbf{k}| \approx 2k_F)}{M_{34}(|\mathbf{k}| \approx 2k_F)} \approx \frac{1}{\mathbf{\Pi}(|\mathbf{k}| \approx 2k_F)}. \quad (47)$$

The two contributions from Eqs. (40) and (41) together give, in real space,

$$\frac{\delta n_i}{n_0} = x \sum_j \left(c_1 \frac{e^{-r_{ij}/\xi}}{\xi^{(d-3)/2} (r_{ij})^{(d-1)/2}} + c_2 x [\mathbf{\Pi}^{-1}]_{ij} \right) \varepsilon_j, \quad (48)$$

where r_{ij} is the distance between sites i and j , and c_1 and c_2 are constants that depend on t, t', J and x .

We stress that in the full solution of the linearized equations in which $\delta\chi_i \neq 0$, the structure of Eq. (33) is still preserved, with the factor M_{33}/M_{34} being replaced by a long combination of several M_{ij} elements, which, however, has a *finite negative $\mathbf{k} \rightarrow 0$ limit and a singularity at $2k_F$* . Therefore, the results of Eqs. (40), (41) and (48) remain valid in the general case. The spatial charge fluctuations for three impurities and the PS in the normal state in the full solution are shown in Fig. 3 both in the absence and in the presence of strong correlations. Note how the non-local part is down by an additional factor of x as compared to the local part [see Eqs. (41) and (48)].

[1] P. Lee, N. Nagaosa, and X. Wen, Rev. Mod. Phys. **78**, 17 (2006).

[2] The usual choice $\tilde{J} = \frac{1}{4}J$ does not change the analytical results and would give rise to hardly noticeable changes in the numerical plots.